Hierarchical Optimization: Fast and Robust Multiscale Stochastic Reconstructions with Rescaled Correlation Functions

Marina V. Karsanina[1,2,*] and Kirill M. Gerke[1,2,3,4,5,†]
[1]Schmidt Institute of Physics of the Earth of Russian Academy of Sciences, Moscow 107031, Russia
[2]Institute of Geospheres Dynamics of Russian Academy of Sciences, Moscow 119334, Russia
[3]Dokuchaev Soil Science Institute of Russian Academy of Sciences, Moscow 119017, Russia
[4]Kazan Federal University, Kazan 420008, Russia
[5]Moscow Institute of Physics and Technology, Dolgoprudny 141701, Russia

(Received 20 September 2018; published 28 December 2018)

Stochastic reconstructions based on universal correlation functions allow obtaining spatial structures based on limited input data or to fuse multiscale images from different sources. Current application of such techniques is severely hampered by the computational cost of the annealing optimization procedure. In this study we propose a novel hierarchical annealing method based on rescaled correlation functions, which improves both accuracy and computational efficiency of reconstructions while not suffering from disadvantages of existing speeding-up techniques. A significant order of magnitude gains in computational efficiency now allows us to add more correlation functions into consideration and, thus, to further improve the accuracy of the method. In addition, the method provides a robust multiscale framework to solve the universal upscaling or downscaling problem. The novel algorithm is extensively tested on binary (two-phase) microstructures of different genesis. In spite of significant improvements already in place, the current implementation of the hierarchical annealing method leaves significant room for additional accuracy and computational performance tweaks. As described here, (multiscale) stochastic reconstructions will find numerous applications in material and Earth sciences. Moreover, the proposed hierarchical approach can be readily applied to a wide spectrum of constrained optimization problems.

DOI: 10.1103/PhysRevLett.121.265501

Spatial correlation functions (CFs) are universal structure descriptors utilized in a multitude of research areas: statistical physics and material sciences [1–4], material design [5,6], astrophysics [7], rock physics [8–10], soil science [11–13], food engineering [14], environmental studies [15], biological studies [16,17], and hydrogeological studies [18] to name a handful. This popularity can be explained by a number of important properties and practical usability. First, an extensive theoretical background relating to spatial structure and CFs, as well as macroscopic physical properties have accumulated over the last 60 years [1]. Second, the knowledge of CFs for a given material provides a possibility to recover its structure using the so-called stochastic reconstruction procedure [19–21], which is a widely useful application [1,5,6,9,10,12–21]. Third, some CFs can be obtained experimentally from *in situ* measurements, such as x-ray tomography [22], nuclear magnetic resonance [23] and small angle x-ray or neutron scattering (SAXS or SANS) [24], or even fused with direct imaging information for reconstruction purposes [25–28]. Finally, based on stochastic reconstructions and the rescaling property of correlation functions one can fuse multiscale images into a single image [29,30], thus solving a long-standing conundrum of field-of-view versus imaging resolution trade-off, specific for any experimental setup.

Despite the numerous powerful aforementioned applications, stochastic reconstructions based on CFs have been criticized from the viewpoint of other reconstruction techniques such as multiple-point statistics (e.g., [31]) or machine learning (e.g., [32]) based methods. Usually, identified weaknesses include low accuracy (due to insufficient information contained in utilized CFs) and high computational cost. Indeed, starting from the seminal work of Yeong and Torquato [21] based on simulated annealing [33], the quality of reconstructions suffered from decreased [34] or overestimated [29] connectivity (depending on the structure and phase ratio of the reconstructed material), artificial anisotropy [35], inability to address anisotropy effectively, etc. Since then, the majority of the problems have been resolved; e.g., the introduction of cluster function into stochastic reconstruction has allowed for the attainment of an unprecedented accuracy [36], usage of directional CFs solved the problem of anisotropy [37–39]. Moreover, the work of Gommes *et al.* [40,41] established a workflow to access the information content of any set of the correlation function for a given structure, thus, providing a basis to choose CFs needed for a problem at hand. Most importantly, it is now rigorously confirmed that only the first moments of the CFs contain most of the information [36,41,42], thus, justifying the use of two-point statistics which sufficiently

 © 2018 American Physical Society

minimizes computational efforts. As the usual aim of stochastic reconstruction is not to recreate the exact copy [43], but merely create a statistical copy with similar macroscopic properties [1,44], approximately 50%–70% of the information content may suffice for successful outcomes [41]. The less than 100% percent information poses a challenge to CF-based reconstructions preferential annealing to less desirable ground states also referred to as degenerate states [41,45]. The second major problem of computational efficiency, mainly arising due to the slowness of the simulated annealing optimization [33], was mitigated partially by frozen-state annealing [46] and its later modifications [47,48]. These methods first anneal the coarsest features of the structure and then freeze them during a further annealing of the finer details. The overall computational gains are partially offset by the complexity of the freezing protocol and coarse-fine grid jumps, moreover, this approach needs the image of the original structure and, thus, is unable to function based on a set of CFs alone (which is a prerequisite to utilize, for example, SAXS measurements). Still, the frozen-state annealing idea is useful, as it also helps to circumvent the degenerate states issue by starting with coarser features, i.e., placing first the major features accurately and adding the details later [49].

In this Letter, we propose a novel CF-based reconstruction algorithm that helps to solve the aforementioned general problems and abandon the frozen-state protocol. Using the idea of correlation function rescaling [29], we hierarchically reconstruct the structure starting from its coarser to a finer representation using only input CFs set. Below, we first describe the details of our methodology and with real images demonstrate how it results in faster and more accurate reconstructions. Summarily, we highlight the most important applications and the outlook of potential usage to address other relevant problems.

For the purposes of this Letter, we limit our consideration to 2D binary structures (consisting of two phases), e.g., white pores and black solids in case of porous media. A conventional set of three types of two-point correlation functions will be used: (1) the two-point probability function $S_2(\mathbf{r})$ [1] describing the probability that two points separated by a vector displacement $\mathbf{r}(x_1, x_2)$ between x_1 and x_2 lie in the white phase, and the lineal-path function $L_2(\mathbf{r})$ [50] describing the probability that the whole segment $\mathbf{r}$ lies within the either (2) white or (3) black phase. As a basis, we utilize the modified Yeong-Torquato technique [13,21,38,51]. The structure is assumed statistically homogeneous, so that we can consider $\mathbf{r}$ as a scalar distance between pixels. We calculate $S_2(\mathbf{r})$ and $L_2(\mathbf{r})$ functions in two orthogonal and two diagonal directions, thus, giving 12 independent CFs for each 2D image, which are then used separately during reconstruction [38].

For any set of correlation functions considered in Yeong-Torquato technique, matching correlation functions of a given realization with a target CFs set is based on pixel permutations. If a set of two-point correlation functions used in reconstruction is provided in the form of $f_2^\alpha(\mathbf{r})$, where α is a type of CF and $\mathbf{r}$ is a segment of varying length, the difference between two realizations of the structure can be expressed as the sum of squared differences [21,51]:

$$E = \sum_\alpha w_\alpha \sum_{\mathbf{r}} [f_2^\alpha(\mathbf{r}) - \hat{f}_2^\alpha(\mathbf{r})]^2, \tag{1}$$

where $f_2^\alpha(\mathbf{r})$ and $\hat{f}_2^\alpha\mathbf{r}$ are the values of the correlation function sets for two realizations (where the former represents a reference set while the latter represents current reconstruction state), w_α are weighting parameters chosen based on the input of each CF into energy E for disordered structure [51]. The energy E in Eq. (1) is minimized by the simulated annealing optimization. The Metropolis algorithm is used [52] to determine the probability of accepting any permutation p:

$$p(E_{\text{old}} \to E_{\text{new}}) = \begin{cases} 1, & \Delta E < 0 \\ \exp(-\Delta E/T), & \Delta E \geq 0, \end{cases} \tag{2}$$

where T is the so-called "temperature" of the system, and

$$\Delta E = E_{\text{new}} - E_{\text{old}}. \tag{3}$$

At initialization, the temperature is chosen so that the probability p for $\Delta E \geq 0$ equals 0.5 [21]. The following cooling schedule based on geometrical progression is used:

$$T(k) = T(k-1)\lambda, \tag{4}$$

where k is time step and λ is a parameter smaller than but close to unity ($\lambda = 0.999999$ for all reconstructions presented here). An optimized pixel permutation approach based on interface choices [53] was used. Periodic boundary conditions were applied for CFs evaluation. The reconstruction procedure was terminated after 10^6 consecutive unsuccessful permutations. Thus described reconstruction methodology according to Gerke and Karsanina [51] will be referenced as GK from now on.

The general scheme of the novel hierarchical annealing (HA) method with rescaled correlation functions is shown in Fig. 1. A full set of 12 CFs is computed based on the original 2D cubical image representing an original structure which is the only input data for reconstruction procedure. To test the method on a wide variety of natural and artificial porous media structures we chose three samples (see Supplemental Material [54]): ceramic [55], shale, and sandstone [56]. Each input CFs set is then rescaled by coarsening (removing points) [29] according to a number of rescaling steps $m = 2$ (note that it actually means three hierarchical levels, as at the final scale $m = 0$, see Fig. 1 for explanations). Similar to GK at first coarsest scale a random mixture of pixels is created with a phase ration based on the zeroth moment of CFs. After $10^5 + N^2$ consecutive

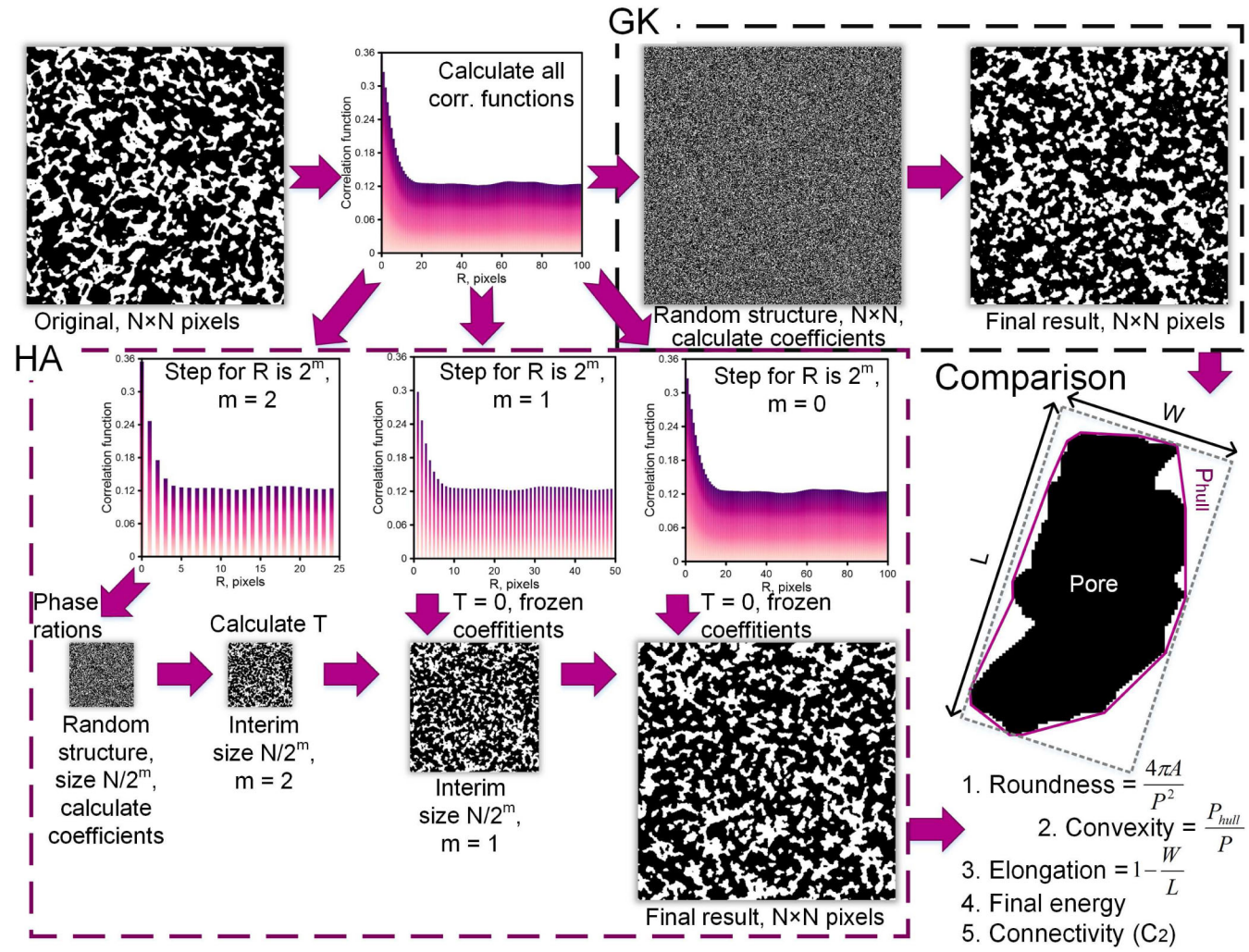

FIG. 1. The general scheme of hierarchical annealing method (HA) and the comparison of its results against nonhierarchical annealing (GK) reconstructions based on five different metrics. On the scheme, N refers to the image width in pixels, m is the hierarchical layer, A is the area of a separate pore object in pixels, P is the perimeter, and P_{hull} is the convex hull, L is the length, and W is the width of the circumscribing rectangle. The final results for HA and GK are the best reconstructions for these methods among five replicas.

unsuccessful permutations are reached, this first annealing step is finalized and each pixel is substituted with four pixels to move to the next hierarchical level. Starting from the second level the temperature T is $= 0$. The latter ensures that permutations of already placed coarse features are penalized leading to a frozen-state annealing type of behavior. Annealing is proceeding with the next scale correlation functions $m = m - 1$ until the same escape condition is reached. The final scale $m = 0$ is annealed until the same criteria as for GK method is reached (to be directly comparable to GK results), i.e., 10^6 consecutive unsuccessful permutations.

Five stochastic replicas are produced for each original 2D image for both GK and HA methodology to explore variability. All replicas are shown in the Supplemental Material [54]. Figure 1 depicts the best ceramic HA reconstruction, Fig. 2 reports the best shale and sandstone replicas best in metrics that were used to assess the accuracy of standard GK and novel HA methods. Comparison metrics [Fig. 1 included (1) final total energy [Eq. (1)]] at the end of reconstruction; (2) the error according to two-point cluster function [computed as squared difference similar to Eq. (1)] [51]; (3) difference in pore morphological parameters [56] between a replica and the original roundness, convexity, and elongation [computed as $\langle\text{original}\rangle/\langle\text{reconstruction}\rangle - 1$, where $\langle\cdots\rangle$ refers to the average for all separate pore objects]. The first metric shows how easily the system can be brought to the ground state, thus, being a direct measure for stochastic reconstruction process effectiveness. The second metric is both a measure of pore connectivity and accuracy, as C_2 is known to add significant additional information to CFs set [36]. The final metric based on separate pore morphology is sensitive to the shape of the reconstructed objects, as well as to the macroscopic physical properties computed based on the reconstruction [56,57].

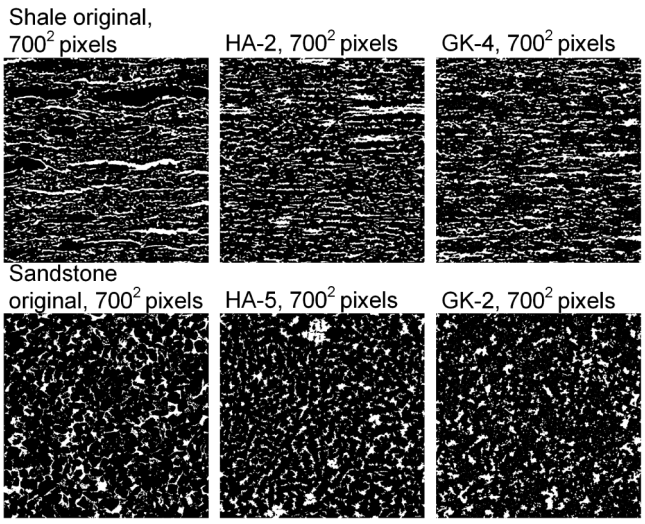

FIG. 2. Shale and sandstone 2D images (from left to right): original images, best HA, and best GK reconstructions.

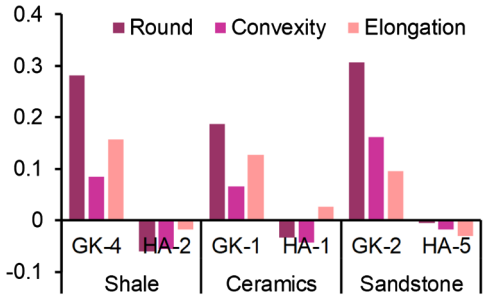

FIG. 3. Comparison of the best reconstructions using HA and GK methods for each of the three original 2D images based on morphological metrics explained in Fig. 1.

For each sample, we chose a single replica (for both GK and HA methods) which is the best in the aforementioned statistics [13]. The results in all metrics for these replicas are shown in Fig. 3 and Table I. The best HA surpass GK replicas along all the metrics used. The final energies terminating the annealing procedures are lower for HA method. Overall connectivity and accuracy according to cluster CF are approximately an order of magnitude better for HA than for GK replicas. Moreover, morphological parameters for pores were significantly better for HA (Fig. 3). All morphological errors for HA are negative (i.e., on average underpredicted, compared to the original), which points to or indicates a drawback in the current implementation pixel permutation choices are more suited for assembling the clusters of pores, while later HA stages require some disassembling to form smaller and single-pixel objects.

To further demonstrate capabilities of the HA method, additional reconstruction results for "classical" testing images are provided in the Supplemental Material [54]. It also includes visualizations of reconstructions at different hierarchical steps m and all final results for three materials discussed here.

While the improvements in the quality of reconstruction can be clearly seen from the above statistics, the most striking difference is actually in CPU time needed to perform reconstructions. On average (computed based on five replicas) about an order of magnitude gain was obtained. Note that the exact comparison of computational efficacy is hampered by the complex influence of annealing termination parameters [29]; i.e., termination by a lower energy threshold or higher number of unsuccessful iterations can only negligibly improve the accuracy while drastically increasing computational effort. Additional research is needed to explore these termination criteria, especially between hierarchical jumps (decreasing m in HA), which may improve the efficacy of the HA method well beyond currently demonstrated gains. Here, we limited our study to the reconstruction of 2D images only, where with increasing m the size of the system decreases as $e^{1/2}$, while for 3D applications such a decrease will be $e^{1/3}$ resulting in even more speed-up compared to nonhierarchical annealing.

From the visual analysis of HA stochastic replicas, one could conclude that reconstructions are still of an imperfect quality. This is definitely due to the insufficient information content of $S_2(\mathbf{r})$ and $L(\mathbf{r})$ directional CFs employed in this work. We argue that this again highlights the importance of the proposed HA technique; with significantly improved computational efficacy one can use as many CFs as necessary to increase the information in CFs reconstruction set to the necessary content. With the inclusion of parallel CFs computation [58] and updating [59] techniques, HA provides a framework to add additional descriptors into the reconstruction procedure, including such computationally heavy CF as $C_2(\mathbf{r})$ cluster function.

Another important aspect of the HA method lies in its ability to reconstruct directly from CFs without any need for an original image, as a prerequisite for the frozen-state type of accelerated annealing procedures. Not only does this

TABLE I. Statistics for the best reconstructions using HA and GK methods for each of the three original 2D images.

	Shale		Ceramics		Sandstone	
The best replica for the sample, number	GK-4	HA-2	GK-1	HA-1	GK-2	HA-3
Cluster CF error	0.000 969	0.000 387 44	0.036 382	0.008 05	0.000 389	1.13E-05
Final energy [according to Eq. (1)]	8.63E-07	7.29E-07	3.98E-06	8.16E-07	2.33E-06	1.9E-06

allow us to reconstruct from multiple (multiresolution) input images (by creating ensemble CFs [30]), but also to utilize experimental CFs obtained using SAXS and SANX, x-ray tomography, or other methods. Additionally, a combination of experimental CFs with those from multiscale (2D) images enables a more accurate reconstruction of submicron and nanoscale materials, e.g., nanomaterials [60], as well as conventional [61] and unconventional [62] hydrocarbon resources. Most importantly, fast HA stochastic reconstructions from CFs alone provide a possibility to store large 3D image data (e.g., about huge geological bodies or tomography data sets) by way of spatial correlation functions [29], so that a structure under question can be recreated easily for any analysis to store statistical descriptors.

One of crucial CF abilities in addition to describing and storing structural information lies with their inheriting multiscale nature [29], that can be measured from images of different resolution or experimentally *in situ* [63]. With orders of magnitude faster HA-based stochastic reconstructions, it is possible to make the multiscale image fusion [29] widely applicable in practice. Note that rescaling of the CFs can be performed not only to coarsen, but also to obtain finer CFs. This can be done by simple interpolation [29,30], or by adding information from higher accuracy sources (such as higher resolution imaging with electron microscopy or nanoscale *in situ* SAXS measurements). That said, HA-based stochastic reconstructions with correlation functions provide a fully multiscale framework necessary to solve field of view–imaging resolution trade-off and, more generally, upscaling or downscaling problem.

In summary, we have presented a novel hierarchical annealing method with rescaled correlation functions, that provides a framework to produce fast, more robust multiscale stochastic reconstructions based on input CFs alone. By mitigating the long-standing computational efficiency problem, the HA algorithm potentially enables us to transform CF-based reconstructions into a widely applicable technique. By significantly reducing the computational burden we allow including more correlation functions into statistical description and reconstruction procedures. Notably, HA should severely reduce the influence of annealing convergence problems after adding numerous CFs, as the coarsest level where the main structure assembling is produced, is much smaller compared to the reconstructed image size.

While in this Letter we focused on 2D binary (two-phase) structures and utilized only a very limited set of CFs, our novel methodology is generally applicable to the reconstruction problem of any complexity. Multiphase materials, such as rocks consisting of numerous mineral and organic phases, or composites, could be reconstructed in the same manner as described here. As 2D image reconstructions allowed for general proof of concept and to perform powerful, yet simple morphological pore analysis, the generalization to 3D reconstructions is straightforward and will be performed in exactly the same manner as for nonhierarchical reconstructions, e.g., [21,51]. With additional effort, the HA-based methodology can be extended to statistically inhomogeneous structures [64], something we completely omitted in the discussion here due to (reasonably considering our original 2D images) the assumption of image stationarity. As already mentioned, a much larger number of correlation functions and other statistical descriptors can be utilized in the reconstruction procedure, corroborating the convergence of the Yeong-Torquato technique as robust after proper weighting as in Eq. (1) [51]. We highlight the importance of solving the problem of information content for other relevant CFs, as only the $S_2(\mathbf{r})$ CF solution exists at the moment [40,41]. The currently discussed implementation of the HA methodology has a few drawbacks, however, namely, the precise criteria to perform hierarchical steps to reduce scale m, as well as an optimal number of such hierarchical steps m, which are expected to further improve the robustness of the reconstruction resulting in a significant speed-up. We hope to address these drawbacks as we research further.

The usage of the proposed hierarchical optimization approach is not limited to stochastic reconstructions alone and can be effectively applied to a wide spectrum of constrained optimization problems.

This research was supported by the Russian Science Foundation Grant No. 17-17-01310. Collaborative effort of the authors is within the FaT iMP (Flow and Transport in Media with Pores) research group and uses its software. We thank our colleagues Dr. Dmitry Korost and Dr. Dina Gafurova for the x-ray microtomography images of porous materials used in this work. We are grateful to two anonymous reviewers for very useful comments.

*marina.karsanina@gmail.com
†kirill.gerke@gmail.com

[1] S. Torquato, *Random Heterogeneous Materials: Microstructure and Macroscopic Properties* (Springer-Verlag, New York, 2002), p. 703.
[2] M. Sahimi, *Heterogeneous Materials I: Linear Transport Properties and Optical Properties* (Springer-Verlag, New York, 2003).
[3] A. Cecen, Y. C. Yabansu, and S. R. Kalidindi, Acta Mater. **158**, 53 (2018).
[4] B. Mortazavi, J. Bardon, J. A. S. Bomfim, and S. Ahzi, Comput. Mater. Sci. **59**, 108 (2012).
[5] Y. Xu, S. Chen, P. E. Chen, W. Xu, and Y. Jiao, Phys. Rev. E **96**, 043301 (2017).
[6] M. Karsanina, K. Gerke, R. Vasilyev, and D. Korost, Math. Model. Comput. Simul. **27**, 50 (2015).
[7] M. Takada and B. Jain, Mon. Not. R. Astron. Soc. **340**, 580 (2003).
[8] J. G. Berryman and S. C. Blair, J. Appl. Phys. **60**, 1930 (1986).

[9] C. Manwart, S. Torquato, and R. Hilfer, Phys. Rev. E **62**, 893 (2000).
[10] H. Izad, M. Baniassadi, A. Hasanabadi, B. Mehrgini, H. Memarian, H. Soltanian-Zadeh, and K. Abrinia, J. Pet. Sci. Eng. **149**, 789 (2017).
[11] E. Sevostianova, B. Leinauer, and I. Sevostianov, Int. J. Eng. Sci. **48**, 1693 (2010).
[12] K. M. Gerke, M. V. Karsanina, and E. B. Skvortsova, Eurasian soil science **45**, 861 (2012).
[13] M. V. Karsanina, K. M. Gerke, E. B. Skvortsova, and D. Mallants, PLoS One **10**, e0126515 (2015).
[14] A. Derossi, K. M. Gerke, M. V. Karsanina, B. Nicolai, P. Verboven, and C. Severini, J. Food Eng. **241**, 116 (2019).
[15] F. Zhao, H. R. Landis, and S. J. Skerlos, Environ. Sci. Technol. **39**, 239 (2005).
[16] J. L. Gevertz and S. Torquato, PLoS Comput. Biol. **4**, e1000152 (2008).
[17] H. Nan, L. Liang, G. Chen, L. Liu, R. Liu, and Y. Jiao, Phys. Rev. E **97**, 033311 (2018).
[18] S. Schlüter and H.-J. Vogel, Adv. Water Resour. **34**, 314 (2011).
[19] J. A. Quiblier, J. Colloid Interface Sci. **98**, 84 (1984).
[20] P. Adler, C. Jacquin, and J. Quiblier, Int. J. Multiphase Flow **16**, 691 (1990).
[21] C. L. Y. Yeong and S. Torquato, Phys. Rev. E **57**, 495 (1998).
[22] H. Li, S. Singh, N. Chawla, and Y. Jiao, Mater. Charact. **140**, 265 (2018).
[23] G. A. Barrall, L. Frydman, and G. C. Chingas, Science **255**, 714 (1992).
[24] C. J. Gommes, Microporous Mesoporous Mater. **257**, 62 (2018).
[25] A. Radlinski, M. Ioannidis, A. Hinde, M. Hainbuchner, M. Baron, H. Rauch, and S. Kline, J. Colloid Interface Sci. **274**, 607 (2004).
[26] H. Li, S. Kaira, J. Mertens, N. Chawla, and Y. Jiao, J. Microsc. **264**, 339 (2016).
[27] H. Li, P.-E. Chen, and Y. Jiao, Transp. Porous Media **125**, 5 (2018).
[28] J.-F. Thovert and P. M. Adler, Phys. Rev. E **83**, 056116 (2011).
[29] K. M. Gerke, M. V. Karsanina, and D. Mallants, Sci. Rep. **5**, 15880 (2015).
[30] M. V. Karsanina, K. M. Gerke, E. B. Skvortsova, A. L. Ivanov, and D. Mallants, Geoderma **314**, 138 (2018).
[31] P. Tahmasebi and M. Sahimi, Phys. Rev. Lett. **110**, 078002 (2013).
[32] L. Mosser, O. Dubrule, and M. J. Blunt, Phys. Rev. E **96**, 043309 (2017).
[33] S. Kirkpatrick, C. D. Gelatt, Jr., and M. P. Vecchi, Science **220**, 671 (1983).
[34] B. Biswal, C. Manwart, R. Hilfer, S. Bakke, and P. Øren, Physica (Amsterdam) **273A**, 452 (1999).
[35] C. Manwart and R. Hilfer, Phys. Rev. E **59**, 5596 (1999).
[36] Y. Jiao, F. H. Stillinger, and S. Torquato, Proc. Natl. Acad. Sci. U.S.A. **106**, 17634 (2009).
[37] H. Kumar, C. Briant, and W. Curtin, Mech. Mater. **38**, 818 (2006).
[38] K. M. Gerke, M. V. Karsanina, R. V. Vasilyev, and D. Mallants, Europhys. Lett. **106**, 66002 (2014).
[39] Y. Jiao and N. Chawla, J. Appl. Phys. **115**, 093511 (2014).
[40] C. J. Gommes, Y. Jiao, and S. Torquato, Phys. Rev. Lett. **108**, 080601 (2012).
[41] C. J. Gommes, Y. Jiao, and S. Torquato, Phys. Rev. E **85**, 051140 (2012).
[42] J. Yao, P. Frykman, F. Kalaydjian, J. Thovert, and P. Adler, J. Colloid Interface Sci. **156**, 478 (1993).
[43] M. G. Rozman and M. Utz, Phys. Rev. Lett. **89**, 135501 (2002).
[44] K. M. Gerke, R. V. Vasilyev, S. Khirevich, D. Collins, M. V. Karsanina, T. O. Sizonenko, D. V. Korost, S. Lamontagne, and D. Mallants, Comput. Geosci. **114**, 41 (2018).
[45] P. Čapek, Transp. Porous Media **125**, 59 (2018).
[46] W. R. Campaigne, P. Fieguth, and S. Alexander, in *Proceedings of the International Conference on Image Analysis and Recognition* (Springer, Berlin, Heidelberg, 2006), p. 41.
[47] D. D. Chen, Q. Teng, X. He, Z. Xu, and Z. Li, Phys. Rev. E **89**, 013305 (2014).
[48] L. M. Pant, S. K. Mitra, and M. Secanell, Phys. Rev. E **92**, 063303 (2015).
[49] S. Chen, H. Li, and Y. Jiao, Phys. Rev. E **92**, 023301 (2015).
[50] S. Torquato, Appl. Mech. Rev. **44**, 37 (1991).
[51] K. M. Gerke and M. V. Karsanina, Europhys. Lett. **111**, 56002 (2015).
[52] N. Metropolis, A. W. Rosenbluth, M. N. Rosenbluth, A. H. Teller, and E. Teller, J. Chem. Phys. **21**, 1087 (1953).
[53] M. Veselý, T. Bultreys, M. Peksa, J. Lang, V. Cnudde, L. Van Hoorebeke, M. Kočiřík, V. Hejtmánek, O. Šolcová, K. Soukup, K. Gerke, F. Stallmach, and P. Čapek, Transp. Porous Media **110**, 81 (2015).
[54] See Supplemental Material at http://link.aps.org/supplemental/10.1103/PhysRevLett.121.265501 for visualizations of reconstructions at different hierarchical steps, all final results for three materials discussed in this Letter, and reconstruction results for "classical" testing images.
[55] K. M. Gerke, D. V. Korost, R. V. Vasilyev, M. V. Karsanina, and V. P. Tarasovskii, Inorg. Mater. **51**, 951 (2015).
[56] X. Miao, K. M. Gerke, and T. O. Sizonenko, Adv. Water Resour. **105**, 162 (2017).
[57] J. R. A. Godinho, K. M. Gerke, A. G. Stack, and P. D. Lee, Sci. Rep. **6**, 33086 (2016).
[58] J. Havelka, A. Kučerová, and J. Jan Sýkora, Comput. Mater. Sci. **122**, 102 (2016).
[59] Y. Ju, Y. Huang, J. Zheng, X. Qian, H. Xie, and X. Zhao, Comput. Geosci. **101**, 10 (2017).
[60] J. J. van Franeker, D. Hermida-Merino, C. Gommes, K. Arapov, J. J. Michels, R. A. J. Janssen, and G. Portale, Adv. Funct. Mater. **27**, 1702516 (2017).
[61] K. Gerke, M. Karsanina, T. Sizonenko, X. Miao, D. Gafurova, and D. Korost, in *Proceedings of the SPE Russian Petroleum Technology Conference, Moscow, Russia*, SPE 187874 (Society of Petroleum Engineers, 2017), DOI: 10.2118/187874-MS.
[62] M. Mastalerz, L. He, Y. B. Melnichenko, and J. A. Rupp, Energy Fuels **26**, 5109 (2012).
[63] C. J. Gommes, J. Appl. Crystallogr. **49**, 1162 (2016).
[64] P. Tahmasebi and M. Sahimi, Phys. Rev. E **91**, 032401 (2015).